Journal of Power Sources 182 (2008) 496–502

Contents lists available at ScienceDirect

Journal of Power Sources

journal homepage: www.elsevier.com/locate/jpowsour

Steam reforming on Ni-samaria-doped ceria cermet anode for practical size solid oxide fuel cell at intermediate temperatures

Mitsunobu Kawano[a,b,*], Toshiaki Matsui[a], Ryuji Kikuchi[a], Hiroyuki Yoshida[b], Toru Inagaki[b], Koichi Eguchi[a]

[a] Department of Energy and Hydrocarbon Chemistry, Graduate School of Engineering, Kyoto University, Nishikyo-ku, Kyoto 615-8510, Japan
[b] Energy Use R&D Center, The Kansai Electric Power Co., Inc., 11-20 Nakoji 3-chome, Amagasaki, Hyogo 661-0974, Japan

ARTICLE INFO

Article history:
Received 21 March 2008
Received in revised form 11 April 2008
Accepted 14 April 2008
Available online 22 April 2008

Keywords:
Solid oxide fuel cell
Methane
Steam reforming
Ni-samaria-doped ceria
Intermediate temperature

ABSTRACT

Direct internal and external reforming operations on Ni-samaria-doped ceria (SDC) anode with the practical size solid oxide fuel cell (SOFC) at intermediate temperatures from 600 to 750 °C are carried out to reveal the reforming activities and the electrochemical activities, being compared with the hydrogen-fueled power generation. The cell performance with direct internal and external steam reforming of methane and their limiting current densities were almost the same irrespective of the progress of reaction in the methane reformate at 700 and 750 °C. The durability test for 5.5 h at 750 °C with direct internal reforming operation confirmed that the cell performance did not deteriorate. The operation temperature of the cell controlled the reforming activities on the anode, and the large size electrode gave rise to high conversion due to the slow space velocity of the steam reforming. Direct internal steam reforming attained sufficient level of conversion for SOFC power generation with methane at 700 and 750 °C on the large Ni-SDC cermet anode.

1. Introduction

Intermediate temperature solid oxide fuel cells (SOFCs) operated at temperatures between 600 and 800 °C have been drawing a great deal of attention because it offers several advantages. The Kansai Electric Power Co., Inc. and Mitsubishi Materials Corp. have been jointly developing intermediate temperature SOFCs since 2001. At present, this development is the practical phase such as 10 kW-class SOFC power generation system [1]. In this development, electrolyte-supported planar-type cells with large electrode (120 mm Ø) are used as a single cell fabricated from microstructure-optimized Ni-samaria-doped ceria ($Ce_{1-x}Sm_xO_{2-0.5x}$; SDC) cermet anode.

On the other hand, among various kinds of hydrocarbon fuels, methane is a typical fuel which is an abundant component in natural gas. Steam reforming of methane on the anode in the SOFC chamber can be carried out along different process routes [2–5]. In this case, steam reforming reaction of methane proceeds with water-gas shift reaction followed by electrochemical oxidation of hydrogen and carbon monoxide.

For the reforming reaction system, three types of operation systems can be considered [6]. They are external, direct internal and indirect internal reforming operation. External reforming operation separates the reforming reaction and the electrochemical oxidation. Then, gaseous species reformed at various extents in the temperature-controllable pre-reformer can be supplied to the anode. In the case of direct internal reforming, on the other hand, methane fuel is directly introduced to the fuel cell chamber. This mode is expected to simplify the overall system design. In this case, reforming reaction and electrochemical oxidation reaction simultaneously proceed at the same anode.

Progress of reforming reaction and the consumption of fuels should be different depending on cell size, cell configuration and the operation temperature. Investigation on the characteristics of power generation using electrolyte-supported planar-type cell with large electrode at various operation temperatures is requested to clarify the reforming activities and electrochemical activities at the anode. Moreover, the adaptability of SOFC to methane fuel can be evaluated by supplying various extents of reformed methane to the anode under direct internal reforming and temperature-controllable external reforming conditions. Thus, comparison of these operation modes is beneficial to optimize the system.

* Corresponding author. Energy Use R&D Center, The Kansai Electric Power Co., Inc., 11-20 Nakoji 3-chome, Amagasaki, Hyogo 661-0974, Japan.
Tel.: +81 6 6494 9715; fax: +81 6 6494 9705.
E-mail address: kawano.mitsunobu@e2.kepco.co.jp (M. Kawano).

0378-7753/$ – see front matter © 2008 Elsevier B.V. All rights reserved.
doi:10.1016/j.jpowsour.2008.04.030

In this study, direct internal and external reforming operations with large Ni-SDC anode at intermediate temperatures are carried out to reveal the reforming activities and the electrochemical activities. The results are compared with the hydrogen-fueled power generation. Furthermore, feasibility of direct internal reforming on the large anode is also investigated to analyze the progress of reactions along the radial direction in relation with the results for the small anode demonstrated previously [7].

2. Experimental

2.1. Cell fabrication process

The fuel cells were fabricated with the similar process described in the previous study [7]. Optimized NiO–SDC composite particles synthesized by spray pyrolysis were used as raw materials of the anode [8,9]. $La_{0.8}Sr_{0.2}Ga_{0.8}Mg_{0.15}Co_{0.05}O_{3-\delta}$ with 200 μm thickness and $Sm_{0.5}Sr_{0.5}CoO_{3-\delta}$ were selected as electrolyte and cathode, respectively.

2.2. Electrochemical characterizations

The diameter of electrode was 120 mm as shown in the photograph of Fig. 1. Air and fuel were supplied from the center of the cathode and anode, respectively (Fig. 1 (b)). The stack unit for this planar cell adopted a seal-less structure in which the unspent fuel and air were exhausted and burned at the outer rim of the stack unit. The cell performance test was carried out in the temperature range of 600–750 °C which was maintained using a plate-heater. Air was supplied to the cathode at a flow rate of 1700 ml min^{-1}. Humidified methane with steam to carbon ratio (S/C) = 3 or hydrogen (H_2–32.2%H_2O) was also supplied to the anode. The flow rates of methane and hydrogen were 85 and 340 ml min^{-1}, respectively. Water vapor was supplied by a pump at a liquid feed rate of 0.20 ml min^{-1} with methane and 0.13 ml min^{-1} with hydrogen, respectively. The piping of this measurement system was heated at 200 °C to avoid condensation of water vapor. The partial pressure of oxygen (pO_2) and gaseous species at the anode were estimated by thermodynamic calculation using MALT software (Version1.0, Kagaku Gijutsu-Sha). Partial pressure of oxygen, pO_2, in the fuel mixture was controlled by the ratio of the fuel and water vapor. In some experiments, the pO_2 for humidified hydrogen was controlled to be the same as that estimated for humidified methane. External steam reforming (Run A and B) and direct internal steam reforming (Run C) of methane was carried out as shown in Table 1. For external steam reforming, humidified methane was supplied to the pre-reformer containing 2 wt.% Ru-Al_2O_3 reforming catalyst (27 cm^3), prior to introduction to the cell. In this case, the temperature of the pre-reformer was set at 750 (Run A) and 450 °C (Run B) to supply the mixture with different levels of the reforming. In the case of direct internal steam reforming, humidified methane was directly supplied to the anode through the by-pass line of the pre-reformer. The gaseous composition in the reformate except for water vapor were measured by micro-gas chromatograph (Varian, SP-4900) before and after the consumption by electrochemical reaction. *I-V* characteristics were measured with increasing current density until the limiting current density appeared as the sharp drop of terminal voltage because of the depletion of fuel species. AC impedance was measured in the frequency range from 100 kHz to 0.1 Hz with an AC amplitude of 17.7 mA cm^{-2}.

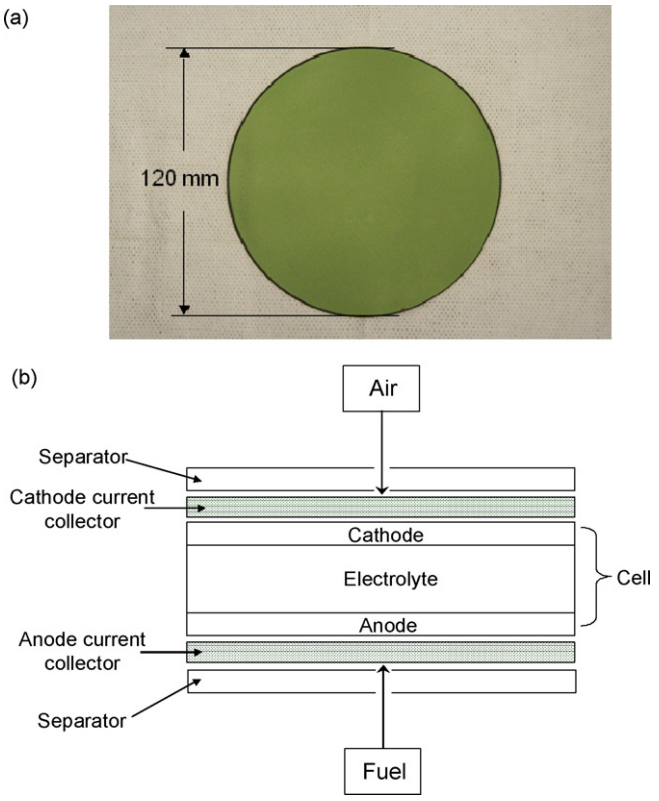

Fig. 1. (a) Photograph of an electrolyte-supported planar-type cell from the anode side before power generation and (b) schematic view of the cross-section of the stack unit.

3. Results and discussion

3.1. Electrochemical characteristics with various steam reformed methane and humidified hydrogen

Power generation of a single cell was tested by supplying the model fuels of external and direct internal steam reform-

Table 1
Gas composition of power generation test

Operation mode	External steam reforming		Direct internal steam reforming
	Run A	Run B	Run C
Temperature of pre-reformer (°C)	750	450	200[b]
CH_4 (%)	8.0 (0.2)[a]	55.9 (32.1)[a]	99.8 (93.3)[a]
H_2 (%)	70.2 (77.1)[a]	35.8 (54.2)[a]	0.2 (5.4)[a]
CO (%)	18.0 (13.9)[a]	0.5 (0.8)[a]	0.0 (0.0)[a]
CO_2 (%)	3.8 (8.8)[a]	7.8 (12.9)[a]	0.0 (1.3)[a]

The concentration of water vapor was excluded.
[a] The value in the parenthesis shows the gas compositions estimated at respective temperatures from the thermodynamic equilibrium.
[b] Methane–steam mixture was supplied to the anode through by-pass line heated at 200 °C in the case of Run C.

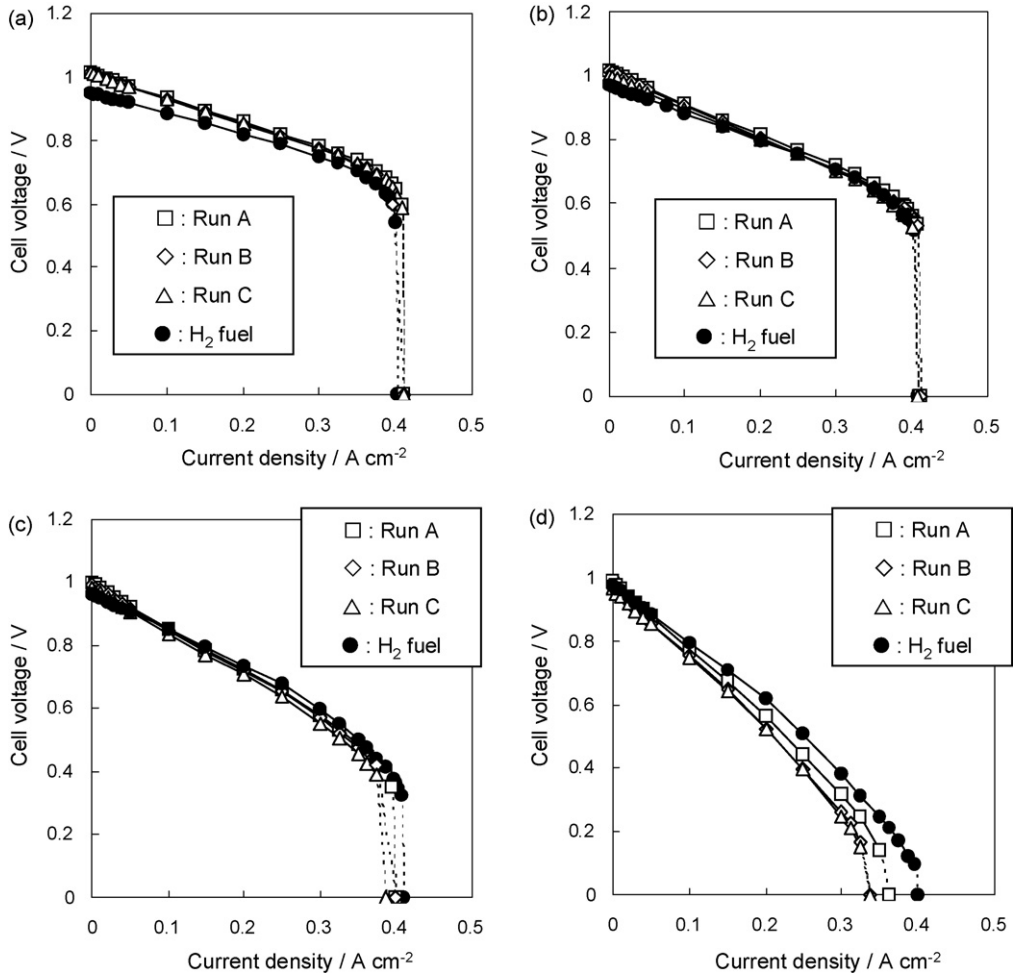

Fig. 2. *I-V* characteristics of a single cell supplied with various reformed methane and humidified hydrogen to Ni-SDC anode at (a)750 °C, (b)700 °C, (c)650 °C, and (d)600 °C.

ing of methane. In the case of external steam reforming, the temperature of the pre-reformer was set at 750 (Run A) and 450 °C (Run B), respectively. In the case of direct internal steam reforming, humidified methane was supplied to the anode through by-pass line heated at 200 °C. The gas compositions employed in this study are summarized in Table 1. These gas compositions did not agree preciously with the thermodynamic estimation at 750, 450, and 200 °C due to the incomplete conversion on the catalyst. However, these gas compositions were stable during the course of the cell evaluation. Thus, the fuel gases with these compositions were introduced to the anode for evaluation of external and direct internal steam reforming of methane.

Fig. 2 shows *I-V* characteristics of the cell supplied with three kinds of gases with different compositions, as well as that with humidified hydrogen. The amount of supplied hydrogen was determined to be four times as much as that of methane because 1 mol of methane is converted to 4 mol of reductants, i.e., 3 mol of hydrogen and 1 mol of carbon monoxide with steam reforming of methane ($CH_4 + H_2O \rightarrow 3H_2 + CO$). The *I-V* performances of the cells and their limiting current densities were almost the same irrespective of the fuel gas compositions at 700 and 750 °C. These results suggest that methane fuel was almost completely reformed on the Ni-SDC anode regardless of the operation runs for external and direct internal steam reforming at 700 and 750 °C. In the operation at 650 °C, the *I-V* performance was lower than those at 700 and 750 °C. The *I-V* curves and limiting current densities depended on supplied fuel conditions. The limiting current density and reduction of *I-V* performance were significantly deviated among the supplied fuels and extent of reforming for the cell operated at 600 °C. At 600 and 650 °C, the limiting current densities were in the sequence of Run C < Run B < Run A < H_2 fuel; i.e., the H_2 fuel led to the highest current density at a given voltage and direct supply of methane led to the lowest one. These results indicate that methane conversions for steam reforming on the Ni-SDC anode at 600 and 650 °C were incomplete and lower than those at 700 and 750 °C. The incomplete conversion of reforming resulted in the relatively large unevenness of each *I-V* performance and limiting current density.

To estimate the fuel concentration for electrochemical oxidation, the limiting current densities were measured by feeding humidified mixed gas composed of various ratios of hydrogen and nitrogen with water vapor. *I-V* characteristics at 750 °C with various concentrations of hydrogen are shown in Fig. 3 (a). Fuel concentrations, [H_2], [CO], and [CH_4], are defined as the percentage fraction of hydrogen, carbon monoxide, and methane in the total gas excluding water vapor, respectively. Fig. 3 (a) and (b) indicates that limiting current density increased linearly in proportion to [H_2]. Fig. 4 shows the dependence of limiting current density under the feed of humidified hydrogen on temperature. The limiting current densities were almost unchanged with the operation temperatures in the range of 600–750 °C. This result suggests that the difference in the

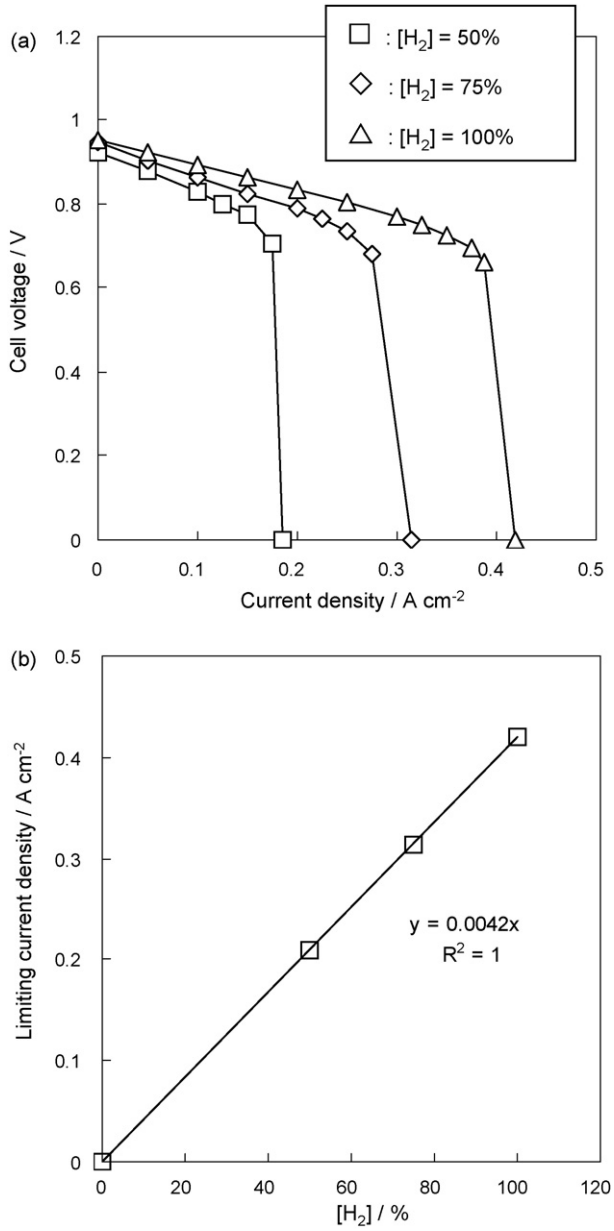

Fig. 3. (a) *I-V* characteristics of a single cell supplied with humidified hydrogen and nitrogen and (b) relationship between limiting current density and concentration of hydrogen at 750 °C.

gas diffusivity across the anode layer did not affect the performance strongly. It is assumed that only hydrogen and carbon monoxide are consumed directly as fuel for electrochemical oxidation reactions, whereas methane could not be directly involved in electrochemical reaction. Reforming may be faster than the direct electrochemical reaction of methane due to low reactivity [10]. Therefore, the sum of $[H_2]$ and [CO] is expected to determine the cell performance and limiting current density. From Figs. 3 and 4, the total concentration of reductant ($[H_2]+[CO]$) at the overall anode could be estimated from limiting current densities in the measurement of *I-V* characteristics in Fig. 2. The calculated results in Fig. 5 indicates that the sum of $[H_2]$ and [CO] at limiting current density was constant at *ca.* 93% over 700 °C. Below 650 °C, however, the sum of $[H_2]$ and [CO] with the supplied fuel condition of Run A–C was lower than that of hydrogen fuel. As shown in Table 1, the concentrations of methane $[CH_4]$ in supplied fuel were 55.9% for Run B and 99.8% for Run C, while that was only 8.0% for Run A. These relatively high $[CH_4]$ correspond to the low reductant concentration for Run B and C below 650 °C. The dependence of limiting current density on the operation temperature implies that methane was completely reformed at 700 °C or higher temperatures under the discharge condition, while reforming was incomplete at or below 650 °C. It is considered that the operation in the range of 700–750 °C realizes the complete direct internal steam reforming on the anode.

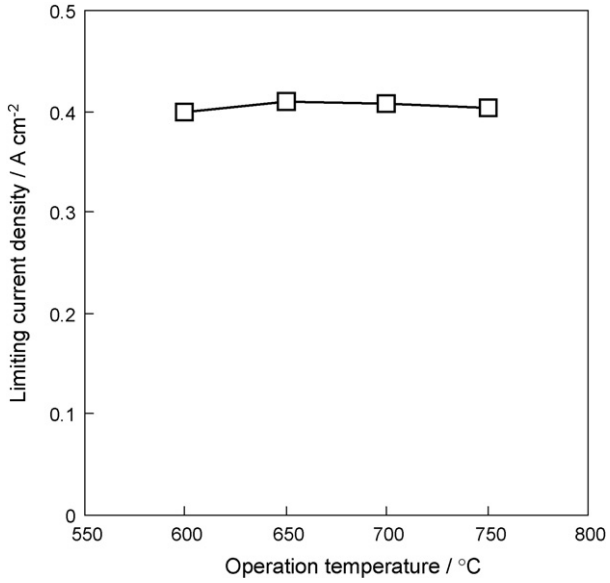

Fig. 4. Dependence of limiting current density on operation temperature for a single cell supplied with humidified hydrogen (H_2–32.2H_2O).

AC impedance spectrum was measured for the cell. As described in the previous report [7], the impedance of the overall cell reflected mainly that of the anode because of the small polarization resistance of the cathode [11]. Fig. 6 shows a typical impedance spectrum

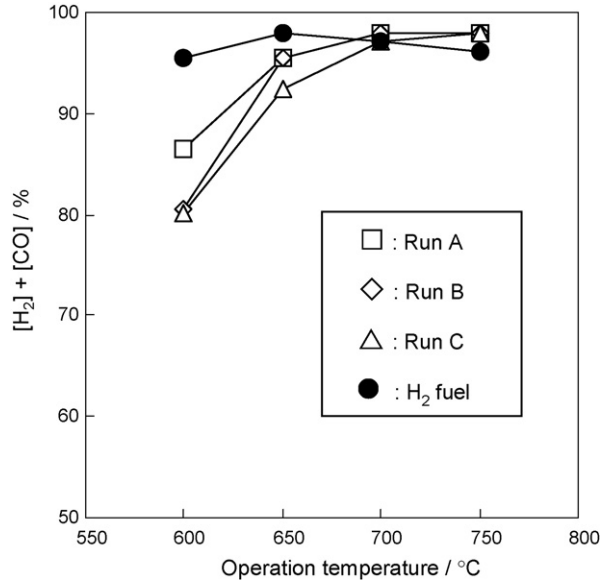

Fig. 5. Relationship between calculated $[H_2]+[CO]$ from limiting current density and operation temperature for a single cell supplied with reformed methane and humidified hydrogen.

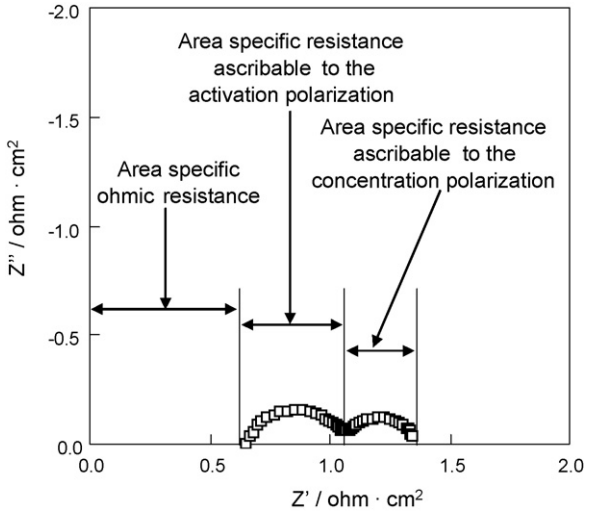

Fig. 6. A typical impedance spectrum of a single cell at 650 °C supplied with humidified methane (Run C) measured at a current density at 0.1 A cm^{-2}.

for a single cell at 650 °C under humidified methane fuel (Run C) at a current density at 0.1 A cm^{-2}. The impedance spectrum was composed of high- and low-frequency semicircles which can be attributed to the resistances for the activation and concentration polarization, respectively [12]. In addition, the high frequency intercepts could also be ascribed to the ohmic resistance of the cell. Then, each resistance was evaluated from the impedance spectra as a function of fuel utilization which is calculated from discharge current and fuel supply.

Fig. 7 shows the area specific ohmic resistance as a function of fuel utilization. The area specific ohmic resistance was almost constant versus fuel utilization and supplied fuel, and increased gradually as the operation temperature was reduced. This dependence of the ohmic resistance on operation temperatures is reasonable because of the Arrhenius-type dependency of conductivity for electrolyte.

The area specific resistances of high frequency semicircles which are ascribable to the activation polarization are plotted in Fig. 8. As the operation temperature was reduced, the resistance for the activation polarization increased due to the positive temperature dependence of catalytic activities of electrodes. The resistances for the activation polarization were gradually reduced with an increase in the fuel utilization. The similar effect was reported previously [13–16], and was ascribed to the promotion of the transport of oxide ions at electrodes under discharge conditions. It is considered that the large heat generation under the higher fuel utilization could enhance the electrochemical reaction at the anode.

As shown in Fig. 9, the resistances of low frequency semicircles ascribable to the concentration polarization were almost constant irrespective of the fuel gas compositions at the fuel utilization below *ca.* 30%. At high fuel utilizations over *ca.* 60%,

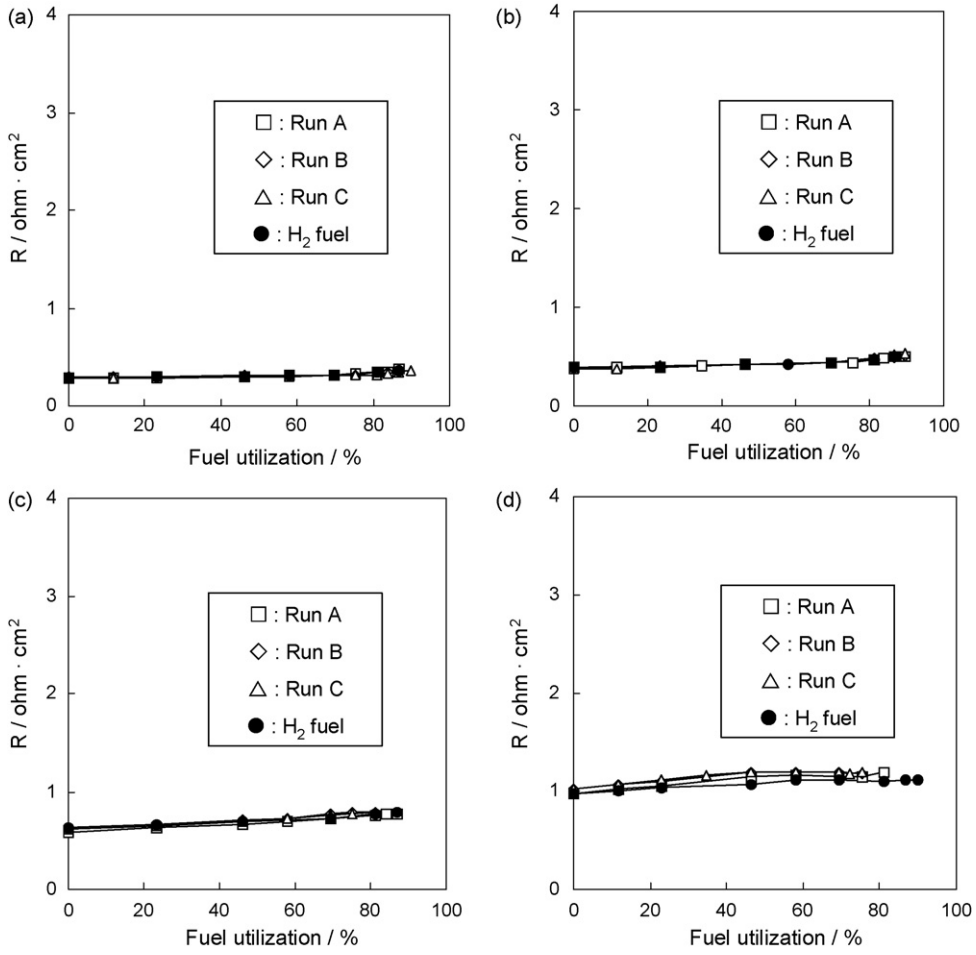

Fig. 7. Relationship between the area specific ohmic resistance and the fuel utilization at (a) 750 °C, (b) 700 °C, (c) 650 °C, and (d) 600 °C.

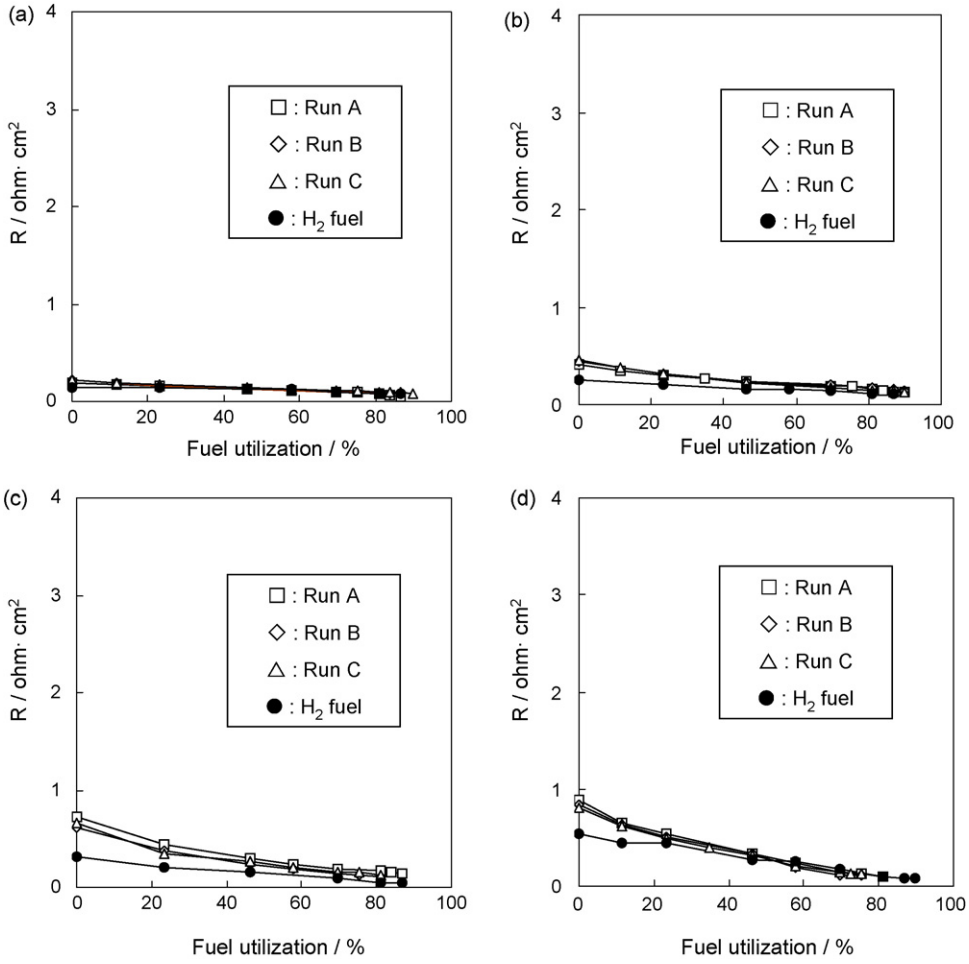

Fig. 8. Relationship between the area specific resistance of high frequency semicircle and the fuel utilization at (a) 750 °C, (b) 700 °C, (c) 650 °C, and (d) 600 °C.

however, the resistance increased with increasing fuel utilization. Moreover, at low operation temperature of 600 °C, the increase of the concentration polarization became significant at high fuel utilizations over *ca.* 60%. At low operation temperatures, steam reforming of methane is considered to proceed incompletely. Thus, insufficient supply of hydrogen and carbon monoxide is responsible for the high concentration polarization. This temperature dependence of resistance from the impedance analysis reflects the *I-V* characteristics and the progress of reforming at respective temperatures. The concentration polarization at the high fuel utilizations was much larger than the ohmic resistance and the activation polarization (Figs. 7–9). Then, it is important, especially at low operation temperatures, to develop the anode with high reforming activities which should minimize the concentration polarization.

Direct internal steam reforming proceeded sufficiently on the large Ni-SDC cermet (120 mm Ø) at 700 and 750 °C, i.e., no appreciable difference in performance of the cell could be observed from the case of external reforming. The maximum power densities with direct internal steam reforming of methane (Run C) were 225.0 and 261.9 mW cm^{-2} at 700 and 750 °C, respectively. In the case of the smaller anode described in the previous study [7], however, the maximum power densities with direct internal steam reforming of methane were only 111.6 and 143.0 mW cm^{-2} at 700 and 800 °C, respectively. This difference in the performance between the large and the small size anode directly corresponds to the difference in the space velocity for the steam reforming reaction on the anode. Calculated space velocity for the large anode is 4×10^2 times slower than that at the small size anode under the same fuel flow rate. The large electrode is suggested to give the wide reaction area and residence time for complete conversion of methane.

3.2. Durability test of direct internal steam reforming on the large size anode

Since the initial SOFC performance with direct internal steam reforming of methane at 700 and 750 °C was high as described above, the durability test of power generation was carried out for *ca.* 5.5 h at 750 °C (Fig. 10). The cell voltage was stable during the discharge of 0.3 A cm^{-2}. The impedance spectrum at the final stage of the durability test agreed with the initial one. These results revealed that the ohmic and polarization resistances were unchanged during the durability test. After the durability test, a small amount of deposited carbon was observed on the central zone of the anode where methane fuel initially contacted to the anode. However, the deposited carbon did not cause the deterioration of overall cell performance.

These results from this durability test show the feasibility of long time operation with direct internal steam reforming. However, the prolonged durability test should be required to discuss the stability of direct internal steam reforming operation on the Ni-SDC cermet anode.

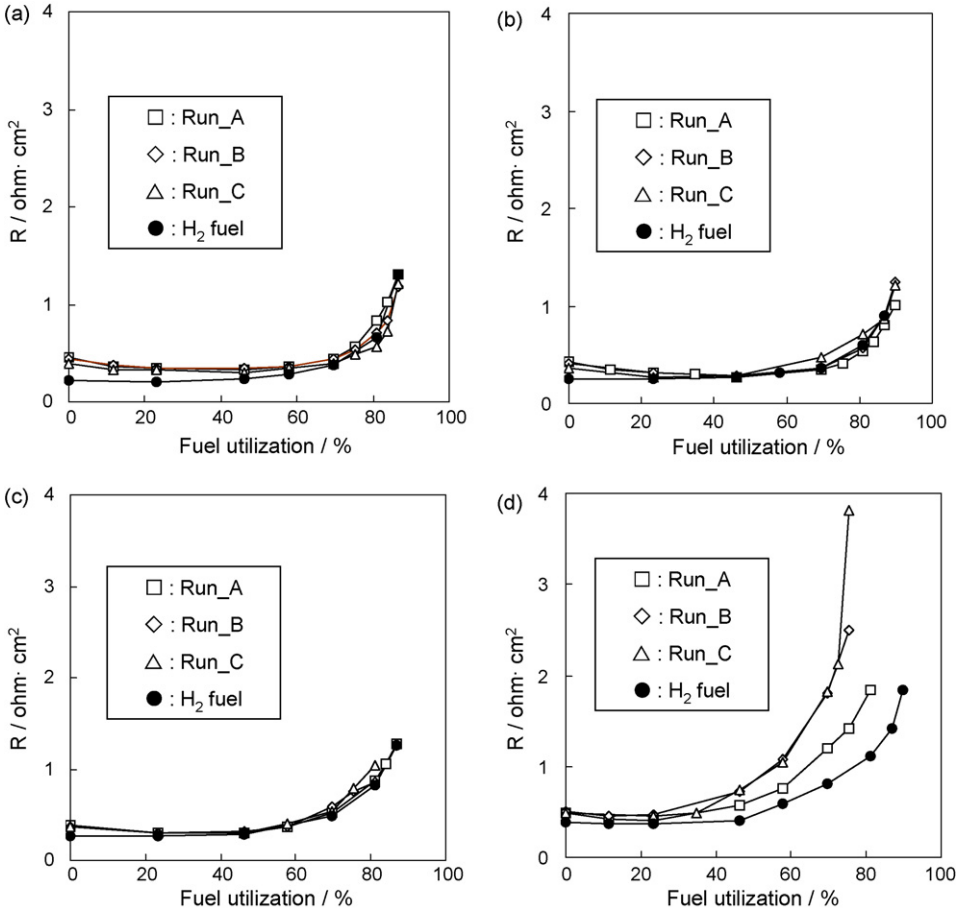

Fig. 9. Relationship between the area specific resistance of low frequency semicircles and the fuel utilization at (a) 750 °C, (b) 700 °C, (c) 650 °C, and (d) 600 °C.

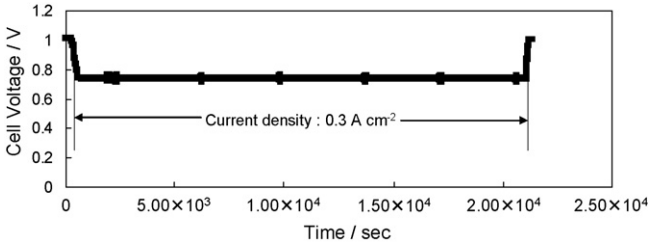

Fig. 10. Stability of the cell supplied with humidified methane (S/C = 3.0) at 0.3 A cm^{-2} at 750 °C.

4. Conclusion

Direct internal and external steam reforming operations using humidified methane fuel on the large Ni-SDC cermet anode (120 mm Ø) of the practically designed cell were carried out. The power generation characteristics were compared for reformed fuel and humidified hydrogen at the operation temperatures from 600 to 750 °C. The cell performance with direct internal and external steam reforming of methane and their limiting current densities were almost the same irrespective of the progress of reaction in the methane reformate at the cell temperature of 700 and 750 °C. However, the performance with direct internal reforming was lower than that with external reforming at the cell temperature of 600 and 650 °C because of the insufficient activity of Ni-SDC for reforming. The cell performance was not deteriorated with an elapse of time for 5.5 h at 750 °C. The operation temperature of the cell controlled the reforming activities on the anode, and the large electrode gave rise to high conversion due to the slow space velocity of the steam reforming. It is concluded that the direct internal steam reforming attained sufficient level of conversion for power generation with methane at the operation temperatures of 700 and 750 °C on the large Ni-SDC cermet anode.

References

[1] M. Shibata, N. Murakami, T. Akbay, H. Eto, K. Hosoi, H. Nakajima, J. Kano, F. Nishiwaki, T. Inagaki, S. Yamasaki, ECS Trans. 7 (1) (2007) 77.
[2] S.H. Clarke, A.L. Dicks, K. Pointon, T.A. Smith, A. Swann, Catal. Today 38 (1997) 411.
[3] A.L. Dicks, J. Power Sources 71 (1998) 111.
[4] O.A. Marina, M. Mogensen, Appl. Catal. A 189 (1999) 117.
[5] M. Boder, R. Dittmeyer, J. Power Sources 155 (2006) 13.
[6] K. Eguchi, in: W. Vielstich, H.A. Gasteiger, A. Lamm (Eds.), Handbook of Fuel Cells—Fundamentals, Technology and Applications, 4, John Wiley & Sons, Ltd., Chichester, U.K., 2003, p. 1057.
[7] M. Kawano, T. Matsui, R. Kikuchi, H. Yoshida, H. Yoshida, T. Inagaki, K. Eguchi, J. Electrochem. Soc. 154 (5) (2007) B460.
[8] M. Kawano, H. Yoshida, K. Hashino, H. Ijichi, S. Suda, K. Kawahara, T. Inagaki, J. Power Sources 152 (2005) 196.
[9] M. Kawano, H. Yoshida, K. Hashino, H. Ijichi, S. Suda, K. Kawahara, T. Inagaki, Solid State Ionics 177 (2006) 3315.
[10] T. Hibino, A. Hashimoto, K. Asano, M. Yano, M. Suzuki, M. Sano, Electrochem. Solid-State Lett. 5 (2002) A242.
[11] T. Ishihara, M. Honda, T. Shibayama, H. Minami, H. Nishiguchi, Y. Takita, J. Electrochem. Soc. 145 (1998) 3177.
[12] S. Primdahl, M. Mogensen, J. Electrochem. Soc. 146 (1999) 2827.
[13] X.J. Chen, K.A. Khor, S.H. Chan, Solid State Ionics 167 (2004) 379.
[14] F.S. Baumann, J. Fleig, M. Konuma, U. Starke, H.-U. Habermeier, J. Maier, J. Electrochem. Soc. 152 (10) (2005) A2074.
[15] K. Huang, J. Electrochem. Soc. 151 (5) (2004) H117.
[16] S. Tao, J.T.S. Irvine, J. Electrochem. Soc. 151 (4) (2004) A497.